Engineering Structures 113 (2016) 89–102

Contents lists available at ScienceDirect

Engineering Structures

journal homepage: www.elsevier.com/locate/engstruct

Experimental investigation on the development of wear in grouted connections for offshore wind turbine generators

Paul Dallyn [a,*], Ashraf El-Hamalawi [a], Alessandro Palmeri [a], Robert Knight [b]

[a] School of Civil and Building Engineering, Loughborough University, Leicestershire, England, United Kingdom
[b] Civil Engineering, E.ON Technologies (Ratcliffe) Limited, Nottingham, England, United Kingdom

ARTICLE INFO

Article history:
Received 10 October 2014
Revised 9 November 2015
Accepted 16 November 2015
Available online 6 February 2016

Keywords:
Grouted connection
Integrity assessment
Offshore structures
Wear development
Wind turbines

ABSTRACT

Relative displacements between grout and steel have been observed in grouted connections used for offshore wind turbine substructures, which appear to be linked to the unexpected settlements that have occurred in some offshore wind farms. A literature review has highlighted a lack of understanding of the implications that this relative movement has on the grout wear. Experimentation has therefore been undertaken to determine the influence of various factors on the wear development, including compressive stress, displacement amplitude, surface roughness and the presence of water, looking at conditions typically experienced by offshore grouted connections. These experiments have indicated that wear of the steel and grout surfaces occur, even at low magnitude compressive stresses. The presence of water has the most significant impact on wear rate, being up to 18 times higher than for the equivalent dry condition. The presence of water can also significantly reduce the coefficient of friction to values lower than typically recommended for evaluation of grouted connections. These findings demonstrate that wear of the grouted connection is likely to occur over the life of this type of offshore structures and should therefore be considered when evaluating their integrity and assessing their behaviour.

1. Introduction

Grouted connections have extensively been used in the oil and gas industry for decades, but in recent years their use has proliferated in the offshore wind industry as an efficient method of joining the monopile (MP), embedded in the sea bed, to the transition piece (TP), which connects to the wind turbine generator (WTG) tower. In comparison to grouted connections used in the oil and gas platforms, offshore WTG connections have considerably lower radial stiffness with pile diameter to thickness ratios greater than 85, compared to 45 typically for oil and gas. However, lower length to diameter ratios exist with WTG connections, having generally 1.5 times pile diameter overlap compared to oil and gas connections with up to six times overlap, and a higher ratio of moment to axial loads with WTG grouted connection typically experiencing twice the moment to axial force compared to a quarter in oil and gas connections. They consist of a larger diameter circular section placed with overlap, of typically greater than 1.5 diameters, over a smaller diameter circular section, with the resultant annulus between the two sections filled with high strength grout. A typical offshore wind turbine foundation example is depicted in Fig. 1.

The concept of a straight-sided sleeved grouted connection without shear keys had been used for over 650 installed monopiles for several commercial offshore European wind farms, representing around 60% of all installations in Europe [1] up until 2011, when the last of the pre-2010 designed foundations were installed. Following the announcement in 2009 of unexpected settlements of the TP relative to the MP in many offshore wind farms, existing grouted connections have required extensive monitoring assessments and remedial works. This has resulted in a shift away from straight-sided grouted connections without shear keys as the primary load transfer mechanism for offshore wind turbine structures.

Site inspections have shown unexpected settlements resulting in hard contact and load transfer between verticality jacking brackets and the top of the MP, which indicate that the connection has an insufficient axial capacity. The capacity initially develops mainly as a shear resistance due to the surface irregularities mobilising friction, but partially due to adhesion between the grout and the steel. As a result of the overturning moment at the base of the tower, however, an increased shear stress as well as compressive stress is created between the grout and the steel and, if the shear stress at that position exceeds the grout–steel friction resistance,

* Corresponding author.
E-mail addresses: P.A.Dallyn@lboro.ac.uk (P. Dallyn), A.El-hamalawi@lboro.ac.uk (A. El-Hamalawi), A.Palmeri@lboro.ac.uk (A. Palmeri), Bob.Knight@eon.com (R. Knight).

http://dx.doi.org/10.1016/j.engstruct.2015.11.028
0141-0296/

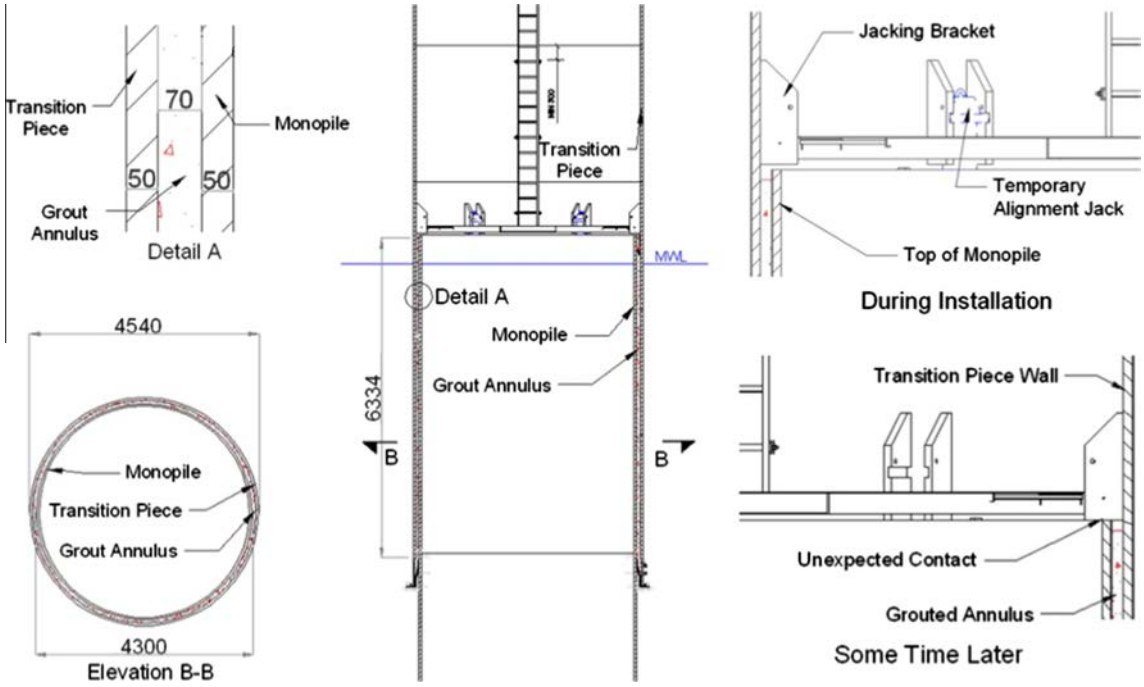

Fig. 1. Typical grouted connection general arrangement.

a relative displacement between the steel and grout occurs. These relative displacements between the MP and the TP are often in excess of 1 mm. They have been observed by subsequent structural condition monitoring, and appear to occur during changes in overturning moment caused by turbine cut-in and cut-off as well as variations in the wind direction and wind speed. The load transfer mechanism is illustrated in Fig. 2.

For full axial capacity of the connection to be mobilised, a relative movement between the steel and grout is required and so small relative displacements should be expected. However, due to the cyclic nature of the loading experienced by the grouted connections, this repeated relative movement has led to degradation of the axial capacity, with a global downward movement in the TP relative to the MP. Importantly, this combination of potentially high compressive stress and relatively large displacements could result in wear at the grout–steel interaction surfaces.

The remedial solutions that have been proposed so far to address this problem typically consist of additional steel brackets and elastomeric bearings installed between the TP and MP. However, the connection still relies on the grout to transfer the bending moments from the TP to the MP and therefore its integrity over the design lifespan of the foundation remains crucial.

Further, the potential for wear, and insufficient axial capacity in non-shear-keyed grouted connections is potentially worsened by water ingress that has been reported at some sites, although not considered in the original design.[1] A literature review undertaken by the authors [2] has revealed that there is a lack of detailed knowledge of the behaviour of the grouted connections, not only for the scale and size of actual structures, but also under the loading and environmental conditions of operation, particularly because the design principles in the existing standards up to 2011 were based on small-scale experimental testing from the oil and gas industry [3–6]. High-strength grout had also only been tested for compressive strength and single axis fatigue by manufacturers and limited testing

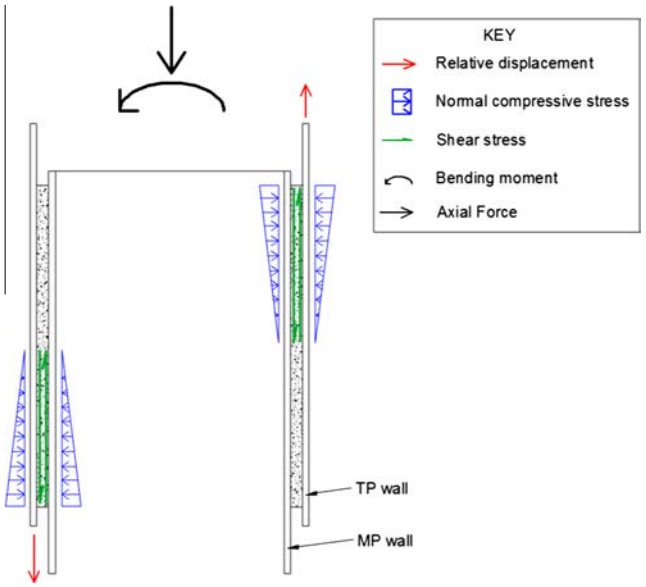

Fig. 2. Load transfer mechanism.

had been undertaken for some of the conditions relevant for offshore wind turbine foundations [7–10].

Overall, the behaviour of the grout–steel interface over long-term service operation is not fully understood within industry and scientific community. Testing has been recently carried out [11–15], but some areas of concern, such as grout wear and environmental conditions, had not been investigated. As a result of the JIP on grouted connections DNV amended DNV-OS-J101 standard [16] to ensure wear failure mode is considered during design. In particular, if wear is occurring and the water ingress provides transportation for the grout material worn down; gaps are likely to form between the grout and outer face of the monopile. This may lead to a lack of fit and some significant dynamic effects on

[1] Due to commercial sensitivity the sites cannot be named.

the structure as the tower oscillates. There is also a risk that the overall length of the grouted connection reduces, due to fracture of the unconfined grout at the top and bottom of the annulus, reducing the lever arm over which the loading is transferred from the TP to the MP, and therefore further increasing the stress in the grout and the steel. With the combination of all these factors, grout wear could be a significant issue for the long-term integrity of the foundation. It is therefore necessary to improve our understanding of the wear failure mode in such situations.

Motivated by the above considerations, this paper details the methodology and results of the experimental campaign undertaken to quantify the wear rates of representative samples of grouted connections under typical offshore conditions, which can then be used to get a more accurate assessment of the wear over the remaining design life of the foundation. In tribology, wear rate is typically defined as volume lost per unit normal load per distance of relative displacement [17]. However, within this research wear rate is quantified as the average change in the measured thickness of the sample per 100 m of cumulative relative displacement ("walked distance") of the interaction surfaces. This definition has been used in order to present the results of our experimental campaign directly into the context of the real-world applications in offshore grouted connections. Cumulative relative displacement is defined as the sum of the relative axial displacements at the grout–steel interface of the sample.

2. Methodology

The aim of this work is to understand the grout wear failure mode under conditions typically experienced during life-time operation of offshore wind turbines. As a necessary first step to achieve this, an experimental protocol has been designed to simulate realistically such challenging conditions. The next two subsections detail the testing apparatus and provide a summary of methodology used for the experimentation.

2.1. Apparatus

The test rig shown in Fig. 3 has been designed in order to allow large variable lateral compressive forces that are operationally representative on the grout/steel interface surfaces (shown by the green[2] line in Fig. 3b), while applying a dynamic vertical displacement to shear the sample along this interface. The vertical load capacity of the testing rig is 160 kN, which allowed testing of samples 150 × 150 mm in size up to maximum compressive stress level of 2.5 MPa, consistent with those indicated by the design load cases, which have subsequently been validated by structural condition monitoring and design checks. The bi-axial stress state produced by this experimental arrangement allowed the reproduction of load conditions which were critical to wear. The tri-axial stress state that is experienced due to ovalisation under bending in operational WTG grouted connections has not been included within this experimentation due to its relative insignificance when determining wear.

Dimensions (Fig. 7) and material properties (Table 3) of the outer and inner steel plates along with the grout have been chosen to be the same as used in typical offshore wind turbine foundations, so that their thickness and stiffness are properly represented, and produced in the same manner as used offshore, resulting in similar surface properties, helping to reduce scaling effects. The test samples were grouted in accordance with the manufacture's recommended procedures and approval, with Densit Ducorit® S5 grout cast onto the inner and outer steel plates using a formwork to ensure containment and dimensions of the grout, shown in Fig. 7. Shear-keys between the outer steel plates and grout ensured de-bonding occurred along the interface between the grout and the inner steel plate, highlighted by the green lines (Fig. 3b). The samples were wrapped in damp cloths and cured for 48 h before being de-moulded and placed in a curing tank for an additional 26 days. Five 100 × 100 mm test cubes and one 150 × 300 mm cylinder were also cast per sample mix to assess the compressive strength, elastic modulus and tensile strength of the grout in each test.

The compressive force applied to the samples could be varied by tightening the compression bolts (Fig. 3). Strain gauges attached to these bolts were calibrated with a load cell before testing commenced, so the compressive stress on the grout can be derived for a given bolt strain and surface area of the grout–steel interaction surface. The compression bolts were re-tightened after each test phase to the required compressive load and the continual monitoring of the strain allowed for compensation during analysis of the data if loss of compression occurred due to wear. The bottom mounting brackets and beam (Fig. 3) have been designed to allow for the horizontal compressive force to transfer wholly from the lateral compression plates to the grouted sample, while still being able to transfer the vertical displacement of the actuator.

To represent the presence of sea water and the implications this may have on the grout–steel interaction, an equivalent solution has been drip-fed onto the top surface of the grout and allowed to drain through the grout/steel interface. The controller software of the testing machine also logged the axial displacements and load required to achieve the desired relative displacements between the grout and steel surface. A vertical Linear Variable Displacement Transducer (LVDT) recorded the actual axial relative displacements between the grout and central steel plate surfaces. Four horizontal LVDTs provided periodic monitoring of the relative lateral displacement between the two outer plates, and therefore any change in thickness of the grout and steel materials if wear occurred was measured. The lateral compression bolt strain was recorded via the same data logger as the displacement sensors, to ensure sufficient numerical data acquisition of the interaction of the steel/grout surfaces. This resulted in 19 channels of data being logged at a frequency of 20 Hz during testing.

In addition to the LVDT measurements, at the end of each phase of testing the accumulated evacuated wear debris was collected and weighed to provide additional information on the loss of material. This was done either through the collection of powder formed above and below the sample in the dry tests or through filtration of the recirculated solution in the wet test. Pre- and post-test Vernier caliper thickness measurements were also taken at 14 circumferential points of each part of the sample at the same points at the beginning and end of each samples' test to determine the total loss of thickness of each of the constituent parts. Visual indicators were also acquired pre- and post-test to indicate the change in surface finish and therefore visual indication if wear is occurring.

2.2. Testing procedure

Site investigations have shown many factors, including steel corrosion, water ingress, surface finish and confinement, can significantly vary between different wind farms, and in the same wind farms between different foundations [2]. To study how each of these factors affect the wear, different samples were prepared and tested, as summarised in Table 1. The levels of corrosion were based on exposure to salt spray for a period of one month resulting in rust grade C to BS EN ISO 8501-1:2007 [18], the Sa 2½ finish to BS EN ISO 8501-1:2007 was achieved by grit blasting of the inner steel plates.

The amplitude of the test cycles was determined from available structural condition monitoring data collected from a typical

[2] For interpretation of colour in Fig. 3, the reader is referred to the web version of this article.

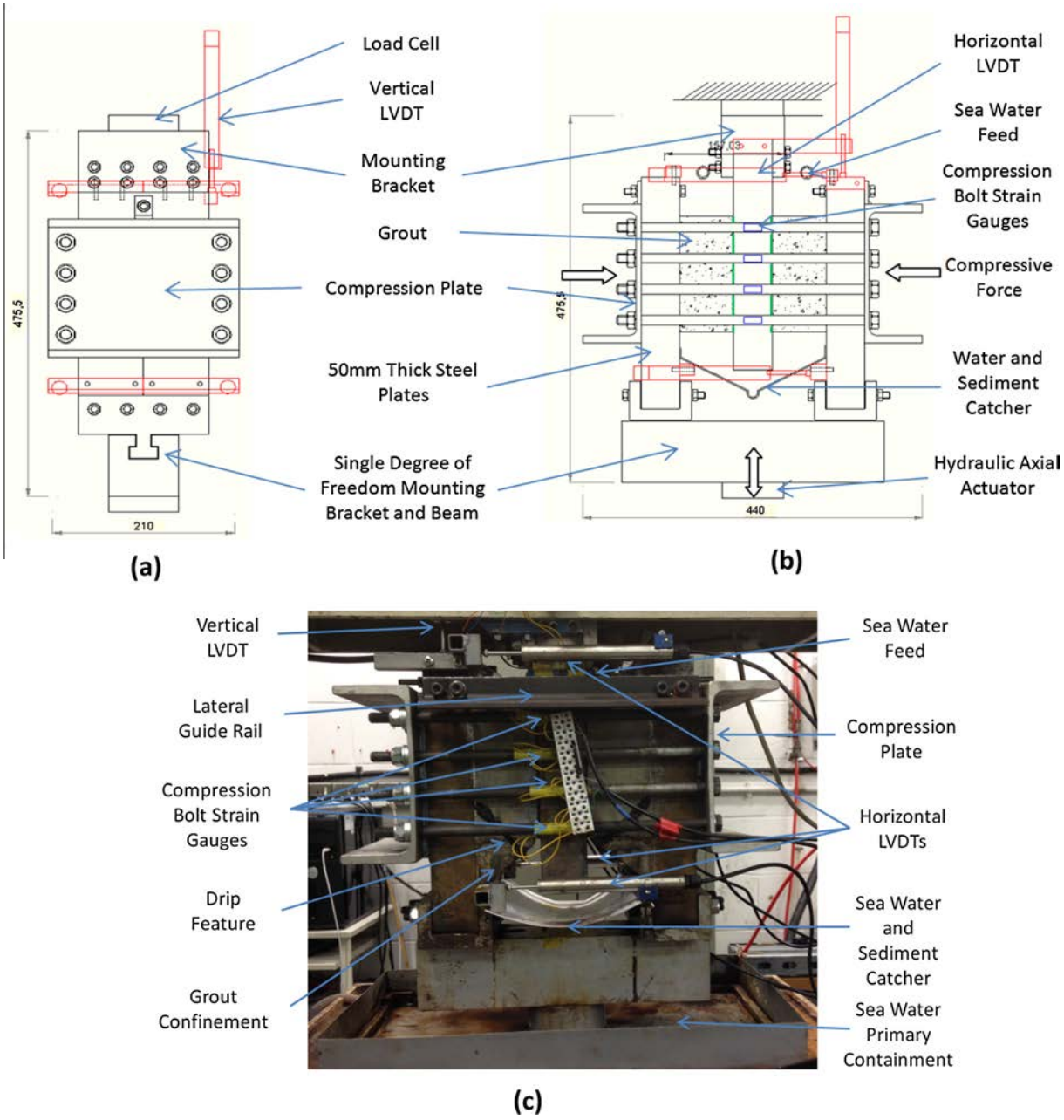

Fig. 3. Experimental test arrangement; side (a), front (b) drawings and front picture of one of the samples ready for testing (c).

Table 1
Sample identification, test matrix.

Sample	Characteristics	Reasoning
S1	Mill Scale, Dry, Unconfined	Test logging equipment & Rig
S2	Mill Scale, Dry, Unconfined	Influence of controller amplitude and frequency
S3	Sa 2.5, Dry, Non-corroded, Confined	Influence of surface finish and higher loads
S4	Sa 2.5, Wet, Corroded, Confined	Influence of water Influence of corrosion (Industry Situation)
S5	Sa 2.5, Wet, Non-corroded, Confined	Influence of water Influence of corrosion
S6	Sa 2.5, Dry, Corroded, Confined	Influence of corrosion (Industry situation/maintained water tightness)

Table 2
Sample adhesion on de-moulding.

Sample	Surface finish	Adhesion
S1	Mill Scale	Medium
S2	Mill Scale	Medium
S3	Sa 2.5, Non-corroded	High
S4	Sa 2.5, Corroded	Low
S5	Sa 2.5, Non-corroded	High
S6	Sa 2.5, Corroded	Low

offshore wind turbine grouted connection affected by insufficient axial capacity. Based on analysis of this data, it was found that maximum peak-to-peak amplitude of relative displacement between the top of the MP and TP of around 1.2 mm was detected,

providing an upper limit of the relative displacement between grout and steel chosen as the primary amplitude for testing. These large-magnitude relative displacements were detected on a daily basis during winter periods, the frequency of which was dependent on the wind conditions. The cycle frequency of 0.3 Hz was determined as the typical natural frequency of the structure being monitored and to allow satisfactory behaviour of the samples without excessive heat generation.

Each sample was subjected to a minimum of seven phases of 8000 cycles at 1.2 mm peak-to-peak axial amplitude for each 0.5 MPa horizontal compressive stress increment, until either the grout failed under shear or the load capacity of the rig was reached. The number of cycles per phase and number of phases per load increment were chosen to ensure sufficient wear would occur to be detectible, allowing wear rates to be determined.

3. Qualitative observations

3.1. Adhesive strength

Samples were de-moulded after 48 h and qualitative observations were recorded on the amount of force required to separate

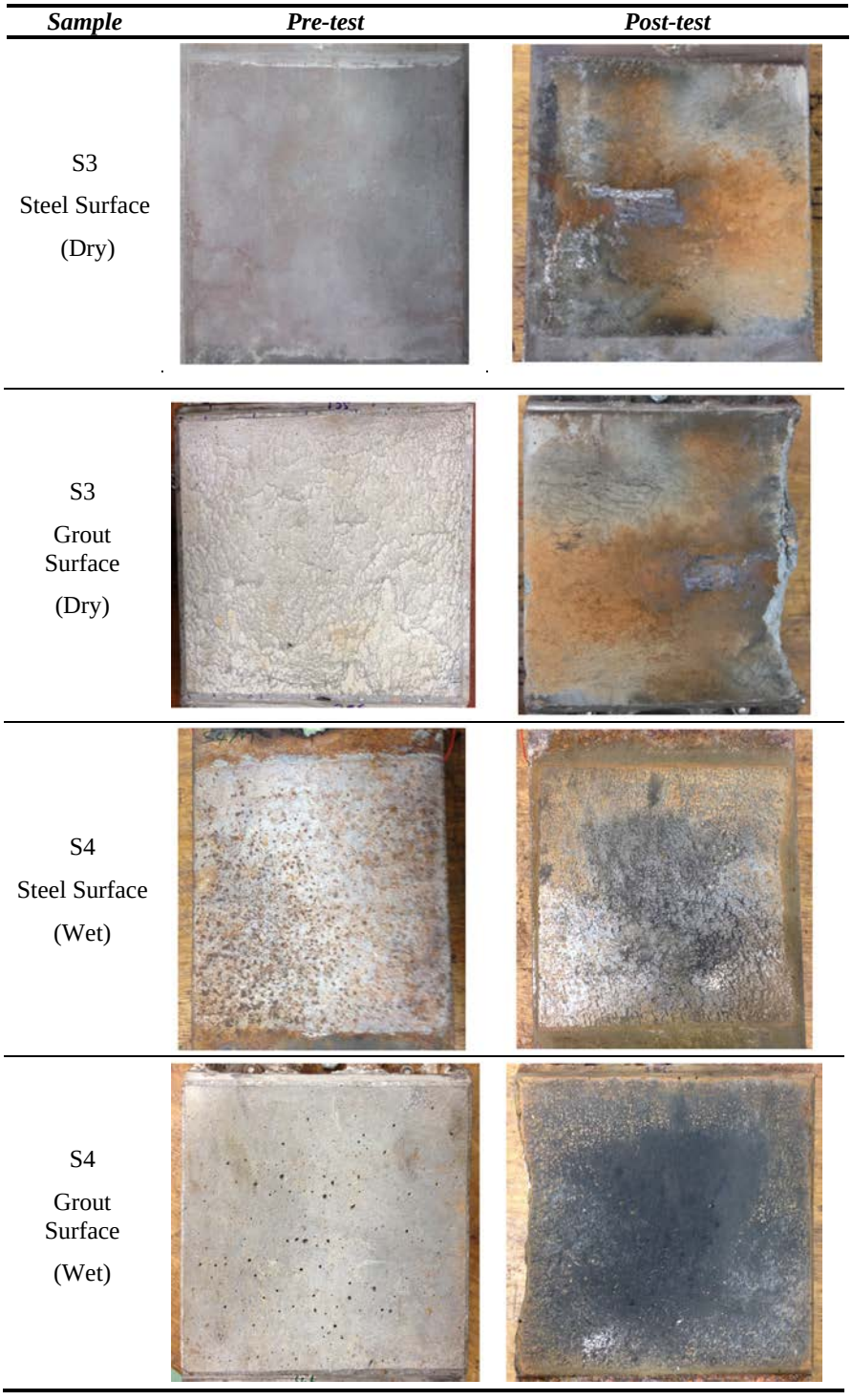

Fig. 4. Pre and post-test surface finishes.

Fig. 5. Post-test grout (left) and steel (right) surfaces of a wet sample.

Table 3
Densit Ducorit® S5 material properties of test samples.

Sample ID	Density (kg/m^3)	Coefficient of variation (%)	28 Day compressive strength (f_c) (MPa)	Coefficient of variation (%)	Tensile splitting strength (MPa)	Elastic modulus (GPa)
S1 and S2	2340 (−3.0%)	0.6	124.7 (0.1%)	1.3	–	–
S3	2420 (0.3%)	0.5	124.0 (−0.5%)	2.6	7.9 (3.6%)	54.50 (1.4%)
S4	2454 (1.7%)	0.7	110.1 (−11.7%)	5.6	7.7 (1.0%)	53.04 (−1.3%)
S5	2433 (0.9%)	0.2	129.5 (3.9%)	2.5	7.5 (−1.6%)	53.90 (0.3%)
S6	2413 (0.0%)	0.2	134.8 (8.2%)	6.1	7.4 (−3.0%)	53.47 (−0.5%)
Average	2412		124.6		7.6	

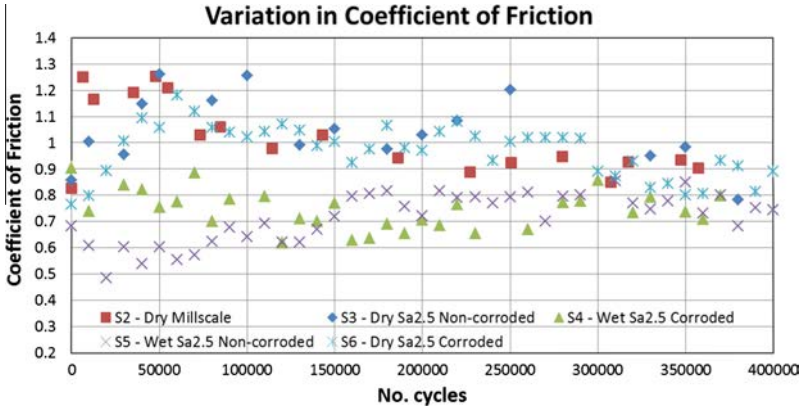

Fig. 6. Measured coefficient of friction.

Table 4
Coefficient of friction statistics.

Sample ID	Characteristics	Mean coefficient of friction	Standard deviation	Coefficient of variation (%)
S2	Mill Scale, Dry, Unconfined	1.02	0.14	13.7
S3	Mill Scale, Dry, Unconfined	1.00	0.13	13.2
S4	Sa 2.5, Wet, Non-corroded, Confined	0.76	0.08	10.1
S5	Sa 2.5, Wet, Corroded, Confined	0.70	0.08	12.4
S6	Sa 2.5, Dry, Non-corroded, Confined	0.97	0.10	10.1

the grout from the inner steel plates. In all but the non-corroded Sa 2½ cases, the 48 h adhesive strength developed at the de-moulding stage was not sufficient to hold the samples together. As reported in Table 2, however, a noticeable difference was seen, depending on the surface finish of the inner steel plate, with high representing forced separation, medium-separation under self-weight and low-separation while de-moulding.

Interestingly, the shot-blasted un-corroded surface finish shows the highest adhesive strength with the shot-blasted corroded surface being the lowest. This experimental observation (which however may need further investigations) may have some direct practical implications. Indeed, given design code equations used to derive the axial capacity of the connection are based on experimental testing which had non-corroded, shot blasted finishes, they did not account for a corroded surface that would be found offshore. Since the steel–grout adhesive strength is part of the total axial bond strength of a connection, the peak bond strength at first slip of a grouted connection in offshore conditions is likely to be lower than expected. These findings align with those of [3], who stated that grouted connections with shot-blasted finishes have a higher axial capacity than those with mill scale finishes. This is likely down to the increased surface roughness of the shot blasted finish and the partially rusty surfaces potentially providing a weaker surface layer. It should be noted that for offshore wind turbine grouted connections where significant bending moments are

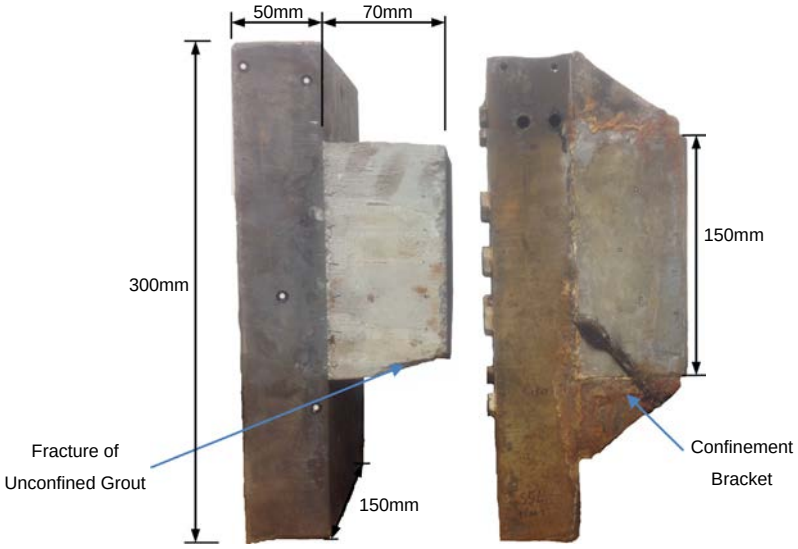

Fig. 7. Picture of unconfined grout (left) and confined grout (right).

transferred and ovalisations occur the resultant tri-axial stress state.

3.2. Surface finish

The pictures in Fig. 4 show the surface finish for some of the samples pre- and post-test.

From Fig. 4 it can be seen by the brown and dark grey areas that in the dry tests, a layer of compressed powder forms on the majority of both the steel and grout surfaces, with greatest thickness, up to 0.4 mm, at the centre of the surfaces. At the top and bottom edges the inner steel plate shows signs of scoring and polishing, indicating that wear is occurring on the steel surface. Moreover an area of metallic sheen can be seen on the grout surface where the layer of compressed powder has been abrading the steel surface.

In the wet test samples, it is evident that there are no signs of compressed powder on either the grout or steel surfaces, with all wear debris appearing to have been evacuated. The interaction surfaces of both the grout and steel were also polished, evident by the reflection of light in the photos and emphasised in Fig. 5, with no signs of the pre-test surface corrosion or finish, indicating that the wetting of the sample is resulting in a fine grinding-like paste being formed by the steel and grout particles that are quickly evacuated.

4. Quantitative results

4.1. Grout properties

The density and mechanical properties of the grout for each mix have been recorded, and a summary of the results is presented in Table 3. The 28-day compressive strength of the Densit Ducorit® S5 grout has been calculated based on the average strength of five 100 mm cubes crushed to the BS EN 12390-3:2009 [19] standard. The tensile strength and elastic modulus are based on tensile splitting and compressive moduli of 150 × 300 mm cylinders to BS EN 12390-6:2009 [20] and BS 1881-121:1983 [21], respectively.

4.2. Average coefficient of friction

Based on the maximum axial force recorded for the given displacement amplitude and compressive force, the resultant coefficient of friction has been calculated based on Eq. (1) for the various surface finishes and environmental conditions.

Table 5
Loss in thickness based on Vernier caliper measurements.

Sample ID	Total walked distance (m)	Loss in thickness (mm)	Coefficient of variation (%)
S3R		−0.04	0.2
S3L		0.11	0.1
S3M		0.16	0.2
S3 Total	1223	0.23	
S4R		0.45	0.2
S4L		0.39	0.2
S4M		0.37	0.1
S4 Total	402	1.21	
S5R		0.41	0.4
S5L		0.38	0.1
S5M		0.31	0.1
S5 Total	490	1.09	
S6R		0.03	0.2
S6L		0.07	0.4
S6M		−0.12	0.1
S6 Total	625	−0.02	

$$\mu = \frac{F}{2R} \tag{1}$$

where F is the axial force, R is the compressive force, μ is the coefficient of friction and a factor of 2 is included to account for the two interaction surfaces of the test arrangement.

It can be seen from Fig. 6 and Table 4 that for all the dry samples (S2, S3 and S6), the coefficient of friction tends to increase over the first 50,000 cycles and then reduces with the total number of cycles experienced tending to the original value. The initial increase could be due to the tolerances of casting and aligning the samples resulting in non-parallel surfaces that over the first 50,000 cycles undergo lapping, removing irregularities and increasing the contact area. The subsequent decrease in coefficient of friction could be due to the grout powder formed, evident in the post sample photos of Section 3.2, forming a sufficiently thick shear layer, where there is particle rotation rather than abrasion in certain areas. The formation of this shear layer is also the likely cause for the results showing limited influence of surface finish on the coefficient of friction between the samples, with values generally being within the variance of the results.

For the wet samples (S4–5), there is an initial decrease in the coefficient of friction, which then tends to re-gain the original

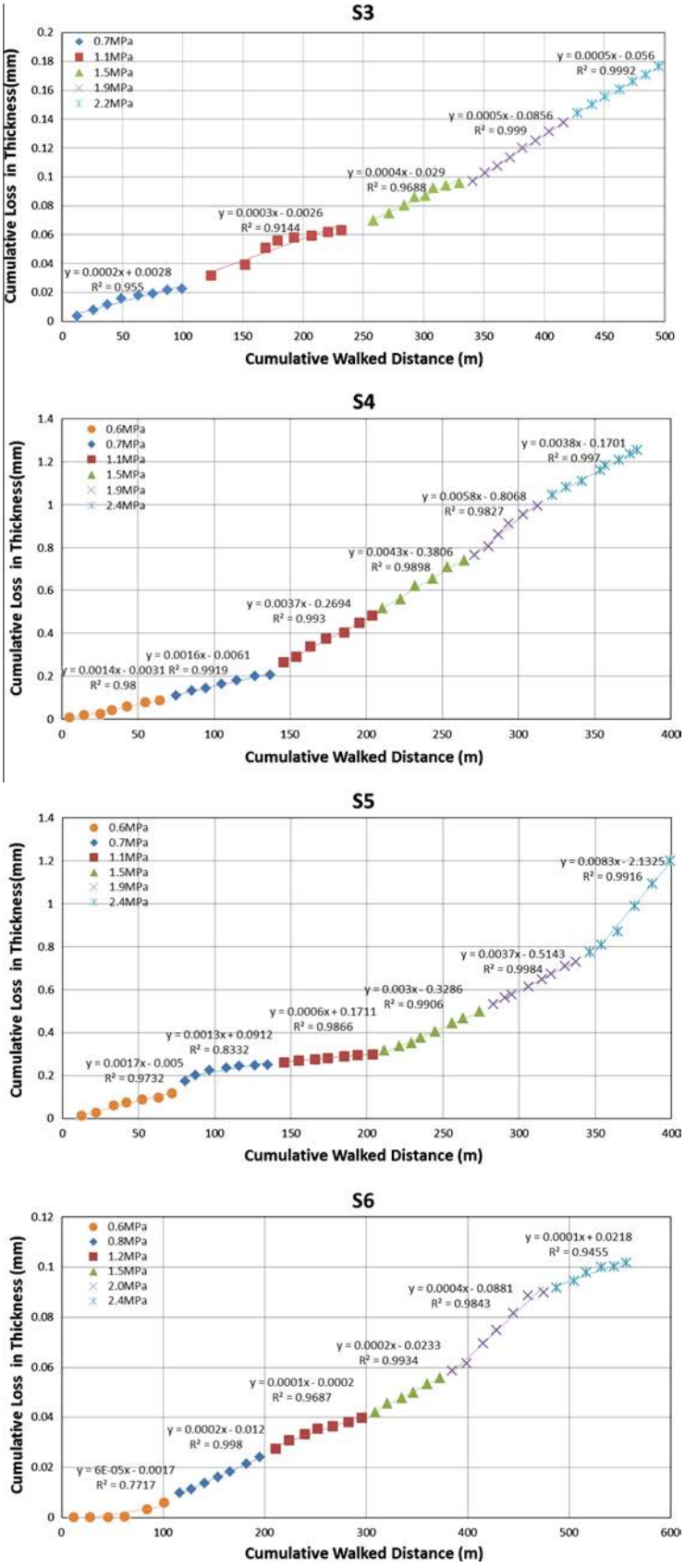

Fig. 8. Loss in thickness based on weight of evacuated material for different conditions.

value. This reduction is likely due to the abrasion of the surfaces resulting in a smooth surface finish, as shown in Fig. 4, as well as the presence of the water acting as a lubricant reducing the friction between the surfaces.

The dry samples indicate coefficients of friction that are above the maximum value of 0.4 to be used in the design of grouted connections in DNV-OS-J101, Section 9 [19], even after 350,000 cycles. The equation presented in Ref. [22] for the interface shear strength due to friction (τ_{kf}) for plain-pipe connections is shown in Eq. (2).

$$\tau_{kf} = \frac{\pi E}{K}\frac{\delta}{R_p} \tag{2}$$

where π is the coefficient of friction, E is the modulus of elasticity of steel, R_p is the pile outer diameter, E is the height of surface irregularities ($0.00037R_p$) and K is a stiffness factor which is dependent on the geometry of the connection and elastic modulus of the grout and steel.

However, the presence of the sea-water equivalent solution in samples S4 and S5 tests clearly shows significantly lower minimum values for coefficient of friction, with values typically 40% lower than the equivalent dry samples for the majority of the test. This indicates that the presence of water will have a stronger influence on the long-term axial capacity of a plain-sided grouted connection than surface finish and presence of corrosion. Although the wet tests indicate that the assumed value of coefficient of friction for design of 0.4 is still conservative for the capacity of grouted connections, the 0.6 recommended for evaluation or modelling of grouted connections [22] may not be conservative. To the best of the authors' knowledge, this is the first time in which the importance of this factor has been experimentally demonstrated.

Based on these test results, it can be recommended that in the design and evaluation of submerged grouted connections a lower value of coefficient of friction is assumed, unless it can be guaranteed that water will not enter at the grout/steel interaction surface over the design life-span of the connection.

4.3. Ultimate failure

Samples S1 and S2 were cast and tested without confinement brackets on the top and bottom of the sample (Fig. 7, left), so to be representative of the very edge of the grouted connection, and both samples have failed with fracture of the grout at compressive stress of 2 and 2.5 MPa respectively. Samples S3 and onwards were cast and tested with confinement (Fig. 7, right), so to allow higher stress levels and represent grout further down the length of the grouted connection, and none of these samples fractured during the cyclic tests. Although further investigations may be needed to confirm these findings, the sharp difference in the performance of confined and unconfined grout seems to indicate that for this type of grout, compressive stress within the very top and bottom of the connection should be limited to less than 2 MPa while in shear, if potential fracture and spalling of the grout is to be avoided under high cycle loading. However, it should be noted that the biaxial stress state of the experimental arrangement is not representative of the tri-axial stress conditions experienced by offshore WTG grouted connections during operation, which could lead to reduced fatigue capacity. Fracture and spalling could result in a reduced connection length, increasing the stress in the remaining grout for a given load.

4.4. Loss in thickness

To quantify the loss in thickness of the samples three alternative methods were used, namely: Vernier caliper; weight of evacuated material; LVDT. The results of these measurements are reported and discussed in what follows.

4.4.1. Vernier caliper measurements

Pre- and post-test thickness measurements of the samples were taken using a Vernier caliper at 14 circumferential points around the left steel and grout (L), right steel and grout (R) and middle steel (M) part of the samples S3 to S6, whose results are listed in Table 5.

It can be seen that for the two dry, samples (S3 and S6) there is minimal loss in thickness and even a slight increase in some parts of the samples. This aligns with the qualitative visual findings reported in Section 3.2, which showed a build-up of a layer of grout powder.

On the contrary, the two wet samples, S4 and S5, show a considerably higher loss of thickness. For instance, comparing samples S3 and S4 reveals that the loss of thickness occurring in the wet sample (S4) was almost six times higher, even though the walked distance for the dry sample (S3) was three times longer. This further confirms the importance of the presence of sea water on the amount of material loss and, based on the Vernier caliper results of our tests, the wet wear rate can be up to 18 times higher than the corresponding dry value.

From the breakdown in loss of thicknesses for the S4 and S5 samples it can be seen that the steel surfaces (S4M and S5M) show about 17% less loss than the grout surfaces. Given that both sides of the inner steel plate interact with the single grout surface on each of the outer parts of the sample, as shown in Fig. 3, the loss in thickness of a single steel surface should be considered half of the value in Table 5. For the dry samples (S3 and S6) a similar ratio is seen although the uneven build-up of the grout powder layer increases the variance in the results.

4.4.2. Evacuated material weight

The material evacuated from the samples has been weighed in order to indirectly determine the loss in thickness of the samples. This has been based on the assumptions that: the steel-to-grout ratio in the collected material is the same as the final measured wear ratio indicated by the Vernier caliper measurements for

Table 6
Comparison of wear rates based on evacuated debris weight.

Sample ID	Test condition	Compressive stress (MPa)	Loss in thickness per 100 m walked distance (mm)	Coefficient of variation (%)
S3	Dry, Sa 2½, Un-corroded	0.7	0.019	12.1
		1.1	0.027	20.8
		1.5	0.035	40.3
		1.9	0.047	34.0
		2.2	0.050	13.5
S4	Wet, Sa 2½, Un-corroded	0.6	0.134	31.4
		0.7	0.215	27.1
		1.1	0.422	27.3
		1.5	0.440	17.4
		1.9	0.548	16.2
		2.4	0.405	28.8
S5	Wet, Sa 2½, Corroded	0.6	0.160	16.2
		0.7	0.254	24.9
		1.1	0.073	15.7
		1.5	0.261	28.0
		1.9	0.349	15.0
		2.4	0.686	22.6
S6	Dry, Sa 2½, Corroded	0.6	0.004	21.0
		0.8	0.017	17.3
		1.2	0.014	19.7
		1.5	0.020	15.1
		2.0	0.034	16.2
		2.4	0.015	17.1

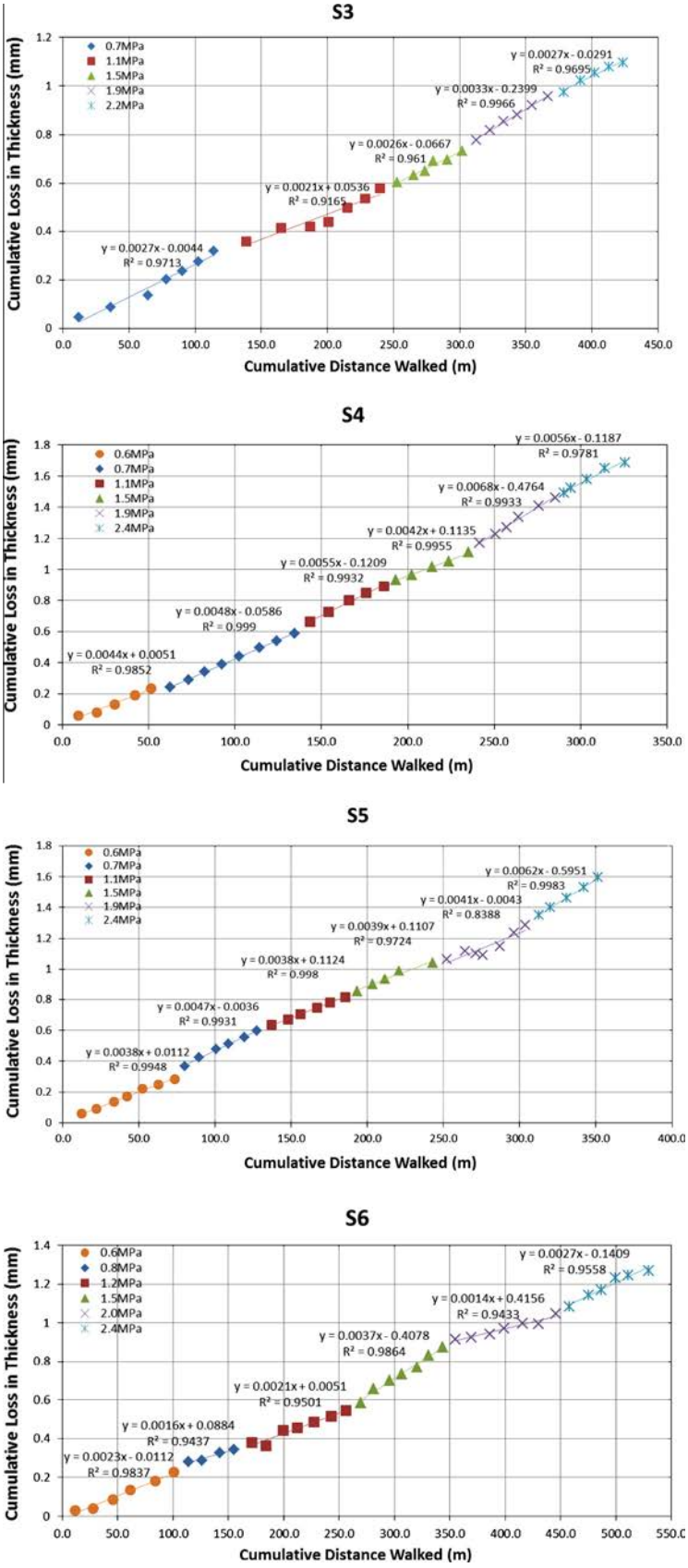

Fig. 9. LVDT measurement of loss of thickness.

Table 7
Comparison of wear rates based on LVDT measurements.

Sample ID	Test condition	Compressive stress (MPa)	Loss in thickness per 100 m walked distance (mm)	Coefficient of variation (%)
S3	Dry, Sa 2½, Un-corroded	0.7	0.26	3.0
		1.1	0.21	2.6
		1.5	0.24	4.6
		1.9	0.35	1.7
		2.2	0.26	3.3
S4	Wet, Sa 2½, Un-corroded	0.6	0.45	7.2
		0.7	0.50	0.9
		1.1	0.55	3.7
		1.5	0.45	8.3
		1.9	0.72	3.9
		2.4	0.60	4.9
S5	Wet, Sa 2½, corroded	0.6	0.33	2.9
		0.7	0.47	7.0
		1.1	0.38	1.3
		1.5	0.43	10.2
		1.9	0.32	16.9
		2.4	0.64	1.3
S6	Dry, Sa 2½, corroded	0.6	0.23	2.7
		0.8	0.12	3.8
		1.2	0.20	6.0
		1.5	0.38	3.8
		2.0	0.16	4.0
		2.4	0.24	6.8

Table 8
Comparison of wear rates.

Sample ID	Test condition	Compressive stress (MPa)	Loss in thickness per 100 m walked distance (mm)	
			LVDT	Weight of evacuated material
S3	Dry, Sa 2½, Un-corroded	0.7	0.26	0.019
		1.1	0.21	0.027
		1.5	0.24	0.035
		1.9	0.35	0.047
		2.2	0.26	0.050
S4	Wet, Sa 2½, Un-corroded	0.6	0.45	0.13
		0.7	0.50	0.22
		1.1	0.55	0.42
		1.5	0.45	0.44
		1.9	0.72	0.55
		2.4	0.60	0.41
S5	Wet, Sa 2½, Corroded	0.6	0.33	0.16
		0.7	0.47	0.25
		1.1	0.38	0.073
		1.5	0.43	0.26
		1.9	0.32	0.35
		2.4	0.64	0.69
S6	Dry, Sa 2½, Corroded	0.6	0.23	0.004
		0.8	0.12	0.017
		1.2	0.20	0.014
		1.5	0.38	0.020
		2.0	0.16	0.034
		2.4	0.24	0.015

samples S4 and S5; density of the grout as in Table 3; density of the steel of 7850 kg/m^3.

For samples S3 to S6, the values of total loss in thickness indicated by the weight of material are all within 0.2 mm of the corresponding values from the Vernier caliper measurements. The slight overestimate of this method is probably due to some of the debris coming from the rig attachments, whose steel powder was also collected. It should also be noted here that the assumption on the wear ratio between the grout and steel can have a considerable effect on the equivalent loss in thickness, due to a large difference in density between the grout and steel (2420–7850 kg/m^3).

Table 9
Comparison of total loss in thickness.

Sample ID	Test condition	Total walked distance (m)	Total loss in thickness (mm)		
			LVDT	Weight of evacuated material	Vernier caliper
S3	Dry, Sa 2½, Un-corroded	1236	2.71	0.20	0.23
S4	Wet, Sa 2½, Un-corroded	402	1.85	1.31	1.21
S5	Wet, Sa 2½, Corroded	490	2.13	1.64	1.09
S6	Dry, Sa 2½, Corroded	625	1.38	0.11	−0.02

Fig. 8 shows that the rate of material loss (indicated by the gradient of the graphs) initially increases with the compressive load and appears to reach a peak before dropping off in all cases except S5. This is more clearly shown in Table 6, where it can be seen that above 2 MPa of compressive stress there is no real increase in wear rate and up to this point there is an approximately linear increase in material loss. The table also shows that the wear rate is around 9–15 times higher for the wet samples for the same surface conditions and compressive stress.

The greater coefficient of variation for the dry samples indicates slightly worse behaviour, which aligns with greater lateral movements being observed during the tests. This appeared to be caused by localised build-up of compressed wear debris in off-centre locations, creating high spots (evident in Fig. 4) with greater resistance to axial movement, causing slight rotational movement around these points.

In terms of surface finish, once again there are marginal differences in wear rates between the corroded and un-corroded samples, with the corroded samples showing slightly lower rates, but within the variance of the data. The limited difference could be justified with the first few cycles of testing, in which the influence of the surface finish is significant, until a powder layer develops and the surface becomes smoothed through abrasion.

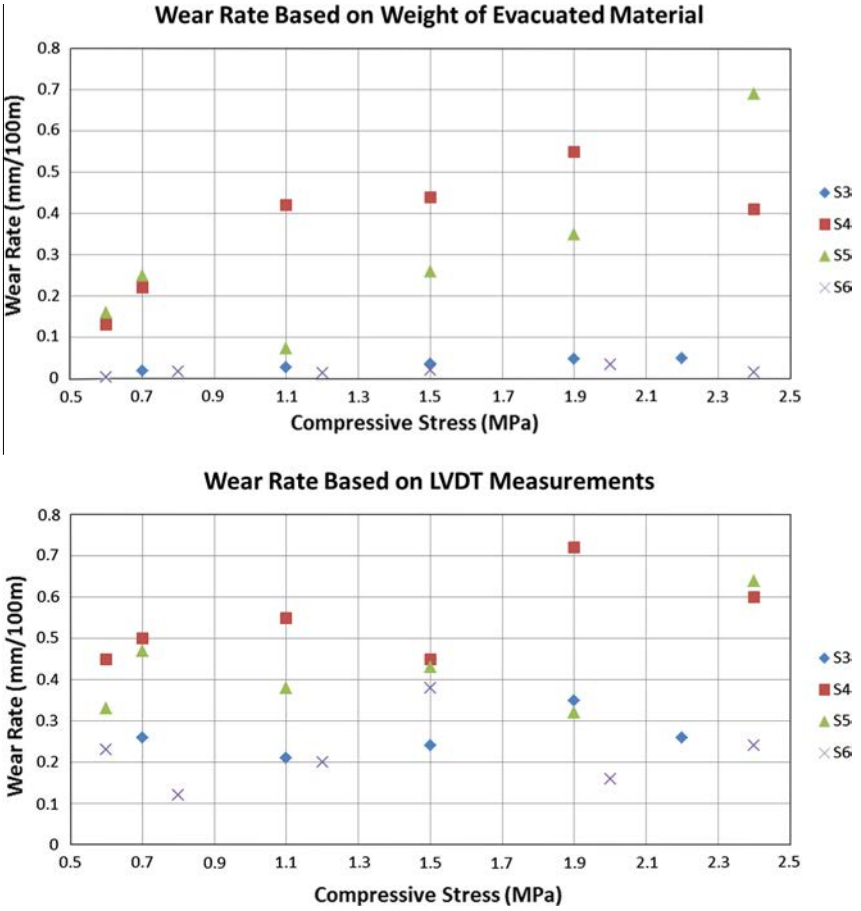

Fig. 10. Wear rates based on LVDT and weight of evacuated material methods.

4.4.3. Linear Variable Displacement Transducer (LVDT) measurements

The horizontal LVDTs provided measurements of the loss in thickness of the sample interface surfaces throughout testing of each sample. Based on the loss in thickness after each phase, the graphs within Fig. 9 have been plotted.

It can be observed that material loss is approximately linear with distance walked with very little difference in gradient for the different compressive stresses on either the dry (S3 and S6) or wet (S4 and S5) shot-blasted finishes, which shows reasonable agreement with the findings of the evacuated material weights. It is however evident that under the wet conditions (S4 and S5), loss in thickness is considerably more, with around 2–3 three times the rate of loss of thickness of the dry test for the various compressive stresses. This is clearly shown in Table 7.

Again, the influence of surface finish on wear rates appears to be a minimal. It is also evident that the total loss in thickness of the samples is up 1.4 times higher than when the weight of evacuated material method is applied to the wet samples, and up to 13 times for the dry samples.

4.4.4. Discussion

The values obtained for total loss of thickness based on the weight of evacuated material generally show good agreement with the Vernier caliper measurements, particularly for the wet tests (see Tables 8 and 9 and Fig. 10), and these values would appear as the most reliable to assess the wear rate.

The horizontal LVDT measurements on the contrary appear to considerably overestimate wear for dry conditions, with the room temperature fluctuations of ±6 °C recorded in the laboratory over one month not justifying such drift in the data, as typical temperature curves for the sensors would allow for an error which is less than 3%.

The slightly more variable lateral motion of the dry samples, mentioned previously, may have also contributed to increase the measured horizontal displacements. The effect of creep of the compression bolts has also been taken into account, based on the average of non-zero values of strain recorded at the end of testing when the compression is removed, and therefore no tensile load is acting on the bolts, and this effect is less than 3.5%.

Taking the gradient of the cumulative relative displacement and loss in thickness results to derive the wear rate may lead to an inaccurate estimation for some of the load levels, where steady state wear was not achieved within the first few test phases of that load increment. An example of this is shown in the results for the 0.7 MPa compressive stress data derived from the weight of evacuated material method for S5 (Fig. 8).

From all the forms of measurements collected as part of our investigations, it is clear that the most significant factor on the wear rate is the presence of water, which at best doubles the wear rate (LVDT method), but at worst could be up to 18 times higher (Section 4.4.1) than for dry conditions. In comparison, the surface conditions of the steel appear to have only a marginal influence, although they are likely to affect initial bond strength of the grout/steel joint.

A possible explanation of such a significant impact of the water presence on the wear rate is the possibility of the wear debris to be evacuated from the interaction surfaces, which is therefore deemed to be critical to the loss in thickness. For dry connections, i.e. when the transition piece is not submerged, this can only happen at the very top or bottom of the connection, which will then

exhibit more loss in thickness. However, for wet connections there is likely to be transportation of the wear debris over the whole length of the connection, and so more significant loss in thickness will occur over the entire length.

It is worth stressing here that, due to the experimental setup, the values of wear rates presented in the study have been obtained with two interaction surfaces because of the nature of the test setup. In the offshore connection, on the contrary, relative displacements tend only to occur at the inner steel–grout surface, due to the smaller area and therefore higher shear stresses. There is therefore only one interaction surface in the actual connections, so the wear rates indicated here should be halved if used to determine the expected wear for typical compressive stresses and environmental conditions of offshore foundations.

5. Conclusions

Unexpected settlements have occurred in large-diameter grouted connections for offshore wind turbines, which can mainly be attributed to: insufficient understanding of the limits and basis of previously used design codes; complex material interaction for a composite connection that experiences a high number of stress cycles; environmental conditions that had not been fully accounted for.

A clear gap has been found in the existing technical literature on the long-term behaviour of plain grouted connections under loading and environmental conditions truly representative of such challenging applications. The testing programme documented in this paper has therefore been undertaken to determine the effects of these conditions on the grout wear failure mode, and to provide input to the foundation integrity assessments of existing foundations.

Our experimentation indicates that wear of the grout and steel interaction surfaces occurs even at low compressive stresses. Wear rates are influenced by the compressive stress with increasing rates up to 2 MPa, after which rates appear to plateau or reduce. The presence of water in the grouted connection, which was not originally considered in design, has been shown to have a significant detrimental effect on wear rate, as it provides a transportation medium for the wear debris. The results show a minimum of twice the wear rate if water is present, but can possibly go up to 18 times, although greater repetition is required to provide significance to these indications. The presence of water also reduces the value of coefficient of friction below levels currently recommended for the evaluation of grouted connections. The influence of displacement amplitude has been investigated at the lower compressive stresses, but no correlation with wear rate was shown, while the influence of the surface finish of the steel is minimal in comparison to the presence of water. Under high cyclic dynamic loading, resulting in relative movements between the grout and steel, it is evident from the testing that fracture of unconfined grout is likely to occur above 2 MPa compressive stress under shear loading. If this results in spalling, the connection length is likely to reduce, increasing the stress in the remaining grout for a given load and exacerbating the problem. The research presented also represents a small but necessary part of the puzzle in regards to the understanding of grouted connections behaviour and occurring mechanisms.

It is evident that wear has potential to influence the structural behaviour of the grouted connection through loss in thickness of the steel and grout, resulting in lack of fit. The influence of the wear should be assessed to determine the likely change in structural response over the life-time of the structure to ensure the natural frequency remains within acceptable limits.

This testing has not been validated by large-scale tests or a full scale WTG grouted connection due to the expense and availability of experimental testing at these scales and the long time period required to detect a significant loss in thickness offshore. Further work is therefore required due to the variation in compressive stresses within the grout over the length and circumference of the grouted connection for a given wind speed, direction and turbine operation. In addition, given these characteristics will vary over the design life of the connection, the amount of wear will inevitably vary around the diameter and across the length of the connection. The value of normal compressive stress experienced will also be influenced by the geometry and therefore radial stiffness of the grouted connection. The values of compressive stress and associated wear rates presented in this research can therefore not just be applied to a single location within the grouted connection, but must account for the variation in loading and geometry of the grouted connection. These aspects of the problem will therefore be assessed as part of further research, with the wear rates determined from the experimentation applied to monitored displacements and compressive stresses within a typical grouted connection, so as to predict the wear experienced over its design life.

Acknowledgments

This study has been developed as part of the first author's EngD (Engineering Doctorate) project, co-sponsored by the ESPRC (the UK Engineering and Physical Sciences Research Council) and E. ON, whose financial support is gratefully acknowledged. The authors would also like to thank ITW Densit for providing the grout.

References

[1] The European Wind Energy Association. The European offshore wind industry key trends and statistics. EWEA; 2010–2013. http://www.ewea.org [accessed 27 November 13].
[2] Dallyn P, El-Hamalawi A, Palmeri, A, Knight R. Wear in large diameter grouted connections for offshore wind energy converters. In: Proceedings of the10th international conference on advances in steel concrete composite and hybrid structures, Singapore; 2012. p. 639–45.
[3] Billington C, Lewis. The strength of large diameter grouted connections. In: Offshore technology conference, OTC, Houston; 1978. p. 291–301.
[4] Karsan D, Krahl N. New API equation for grouted pile to structure connections. In: Offshore technology conference, OTC, Houston; 1984. p. 49–56.
[5] Sele A, Kjeøy H. Background for the new design equations for grouted connections in the DNV draft rules for fixed offshore structure. In: Offshore technology conference, OTC, Houston; 1989. p. 463–74.
[6] Lamport W, Jirsa J, Yura J. Strength and behaviour of grouted pile-to-sleeve connections. J Struct Eng 1991;117:2477–98.
[7] Andersen M, Petersen P. Structural design of grouted connections in offshore steel monopile foundations. Global Wind Power 2004:1–13.
[8] Schaumann P, Wilke F. Design of large diameter hybrid connections grouted with high performance concrete. In: The international society of offshore and polar engineering conference, ISOPE, Lisbon, Portugal; 2007. p. 340–7.
[9] Anders S, Lohaus L. Optimized high performance concrete in grouted connections. Tailor made concrete structures. London: Taylor & Francis Group; 2008.
[10] Schaumann P, Lochte-Holtgreven S, Lohaus L, Lindschulte N. Durchrutschende Grout-Verbindungen in OWEA – Tragverhalten, Instandsetzung und Optimierung, Stahlbau, vol. 79, Issue 9. Berlin (Germany): Ernst & Sohn; 2010. p. 637–47 [Translation].
[11] Veritas Det Norske. Summary report from JIP on the capacity of grouted connections in offshore wind turbine structures. Norway: Det Norske Veritas; 2010.
[12] Lotsberg I. Structural mechanics for design of grouted connections in monopile wind turbine structures. Mar Struct 2013;32:113–35.
[13] Lotsberg I, Serednicki A, Oerlemans R, Bertnes H, Lervik A. Capacity of cylindrical shaped grouted connections with shear keys in offshore structures. Struct Eng 2013;5:42–8.
[14] Schaumann P, Raba A, Bechtel A. Effects of attrition due to water in cyclically loaded grouted joints. In: Proceedings of the ASME international conference on ocean, offshore and arctic engineering, San Francisco, California, USA; 2014.
[15] Veritas Det Norske. Technical note for the certification of grouted connections for offshore wind turbines, revision 0. Norway: Det Norske Veritas; 2011.
[16] Veritas Det Norske. Offshore standard DNV-OS-J101 – design of offshore wind turbine structures. Høvik (Norway): DNV; 2007.
[17] Archard J. Contact and rubbing of flat surface. J Appl Phys 1953;24:981–8.

[18] International Organization for Standardization. ISO 8501-1:2007. Preparation of steel substrates before application of paints and related products – visual assessments of surface cleanliness – Part 1: rust grades and preparation grades of uncoated steel substrates and of steel substrates after overall removal of previous coatings, Geneva, Switzerland; 2007
[19] British Standards Institution. BS EN 12390-3:2009 – testing of hardened concrete Part 3: compressive strength of test specimens. London (England): BSI; 2009.
[20] British Standards Institution. BS EN 12390-6:2009. Testing of hardened concrete Part 6: tensile splitting strength of test specimens. London (England): BSI; 2009.
[21] British Standards Institution. BS 1881-121:1983. Testing concrete Part 121: method for determination of static modulus of elasticity in compression. London (England): BSI; 1983.
[22] Veritas Det Norske. Offshore standard DNV-OS-J101 – design of offshore wind turbine structures. Høvik (Norway): DNV; 2011. 2011.